unambiguously isolated SWNT would have zero neighbors, whereas a nanotube that is clearly part of a large bundle or rope would have multiple neighbors. The small range of neighbor numbers for some samples reflects the general difficulty in unambiguously determining this number using STM imaging alone (similarly, because of finite tip radius, sample curvature, and electronic differences between sample and substrate, using STM imaging alone it is generally difficult to accurately determine the diameter of a given nanotube). Samples 1 through 7 in Table 1 form a natural grouping: these samples were metallic both before and after oxygen dosing. The next two samples, 8 and 9, started out as modest band-gap semiconductors and they remained so. The last group, samples 10 through 17, started out as small band-gap semiconductors and became metallic upon oxygen dosing. Both isolated tubes and tubes with neighbors can be found in this last category. An interesting and suggestive (but not conclusive) observation is that all of the "intrinsically" metallic nanotubes we observed (samples 1 through 7) had nanotube neighbors; we have been unable to find an isolated SWNT that remains metallic upon inert gas cleaning.

Our transport and STS measurements can be interpreted within a consistent picture of oxygen-induced changes in the electronic behavior of SWNTs. The increases in $N(E)$ summarized in Table 1 agree with the oxygen-induced increases in conductivity we have generally measured for films or ensembles of nanotubes. If Table 1 is representative of SWNTs in general, it indicates that SWNT film conductivity might decrease by as much as 50% if all of the oxygen adsorbates could be removed. In contrast, gas adsorption studies on thin metal films generally exhibit conductivity increases as adsorbates are removed, due to surface-sensitive scattering processes (*23*). The STS data also illuminate the change in sign of the TEP. Intrinsically metallic, oxygen-free SWNTs are suggested to have a small negative TEP, whereas oxygen-exposed small band-gap SWNTs may behave as p-type, degenerately doped semiconductors with a relatively large S magnitude. For a sample that is a collection of SWNTs comprising both metals and semiconductors, the overall effects of oxygen doping on S are complex, as one must take into account not only changes in S of individual tubes but also associated changes in tube conductivity that affect the multichannel weighted average of S.

The likelihood of charge transfer from adsorbed oxygen to SWNTs deserves careful investigation. Oxygen is known to have good charge transfer to planar defected graphite, especially in the presence of catalytic metallic particles, which has made graphite the material of choice for fuel cell electrodes. Graphitic microstructures (*24*) and fibers (*18*) can both become hole-doped in the presence of adsorbed oxygen because of oxygen's electron affinity. The SWNT observations may be due to similar effects. However, a key to charge transfer between oxygen and graphite is the presence of defects (*24, 25*). If, as some studies suggest, curvature plays only a small role in adsorption and charge transfer (*26*), any oxygen-induced charge transfer in SWNTs could indicate the presence of on-tube defects, making oxygen sensitivity an ideal way to determine the concentration of defects in carbon nanotubes. In addition, the possibility that oxygen may also adsorb on the inside of nanotubes with open ends should not be overlooked.

References and Notes

1. *Graphite Intercalation Compounds II: Transport and Electronic Properties*, vol. 18, H. Zabel and S. A. Solin, Eds. (Springer-Verlag, New York, 1992).
2. A. C. Dillon *et al.*, *Nature* **386**, 377 (1997).
3. A. Chambers *et al.*, *J. Phys. Chem. B* **102**, 4253 (1998).
4. C. C. Y. Ahn *et al.*, *Appl. Phys. Lett.* **73**, 3378 (1998).
5. V. A. S. Nalimova *et al.*, *Synth. Met.* **88**, 89 (1997).
6. G. T. W. Wu *et al.*, *J. Electrochem. Soc.* **146**, 1696 (1999).
7. S. C. Tsang *et al.*, *Nature* **372**, 159 (1994).
8. K. G. Ayappa, *Langmuir* **14**, 880 (1998).
9. M. Bockrath *et al.*, *Science* **275**, 1922 (1997).
10. S. J. Tans *et al.*, *Nature* **386**, 474 (1997).
11. J. W. G. Wildoer *et. al.*, *Nature* **391**, 59 (1998).
12. T. W. Odom *et. al.*, *Nature* **391**, 62 (1998).
13. For a preliminary report, see P. G. Collins, M. Ishigami, A. Zettl, *Bull. Am. Phys. Soc.* **44**, 1889 (1999).
14. A. Thess *et al.*, *Science* **273**, 483 (1996).
15. Film samples were fabricated by depositing dichloroethane-dispersed SWNTs onto SiO_2 substrates prepatterned with gold electrodes.
16. J. Hone *et al.*, *Phys. Rev. Lett.* **80**, 1042 (1998); L. Grigorian *et al.*, *Phys. Rev. B* **60**, R11309 (1999)
17. P. G. Collins, K. Bradley, A. Zettl, in preparation.
18. N. E. Kobayashi, T. Ishii, K. Kaneko, *J. Chem. Phys.* **109**, 1983 (1998).
19. J. Tersoff and D. R. Hamann, *Phys. Rev. Lett.* **50**, 25 (1983).
20. J. W. Mintmire, B. I. Dunlap, C. T. White, *Phys. Rev. Lett.* **68**, 631 (1992).
21. N. Hamada, S. Sawada, A. Oshiyama, *Phys. Rev. Lett.* **68**, 1579 (1992).
22. M. S. Dresselhaus, G. Dresselhaus, P. C. Eklund, *Science of Fullerenes and Carbon Nanotubes* (Academic Press, New York, 1996).
23. G. Wedler, in *Thin Metal Films and Gas Chemisorption*, P. Wibman, Ed., vol. 32 of *Studies in Surface Science Catalysis* (Elsevier, New York, 1987), sections 2.4, 5.1, and 5.3.
24. L. S. Singer, in *Proceedings of the 5th Carbon Conference* (Pergamon, New York, 1961), vol. 2, pp. 37–50.
25. S. M. Lee, *et. al.*, *Phys. Rev. Lett.* **82**, 217 (1999).
26. P. J. Britto, K. S. V. Santhanam, A. Rubio, J. A. Alonso, P. M. Ajayan, *Adv. Mater.* **11**, 154 (1999).

27. We thank M. L. Cohen and S. G. Louie for useful discussions and J. Hone for help with early TEM experiments. Supported in part by a University of California, Berkeley, Chancellor's Initiative grant; by NSF grants DMR-9801738 and DMR-9501156; and by the Office of Energy Research, Office of Basic Energy Science, Materials Sciences Division of the U.S. Department of Energy under contract number DE-AC03-76SF00098. P.C. acknowledges support from a Helmholz Fellowship and M.I. acknowledges support from the Hertz Foundation.

8 December 1999; accepted 10 February 2000

Hematopoietic Stem Cell Quiescence Maintained by $p21^{cip1/waf1}$

Tao Cheng,[1] Neil Rodrigues,[1] Hongmei Shen,[1] Yong-guang Yang,[2] David Dombkowski,[1] Megan Sykes,[2] David T. Scadden[1]*

Relative quiescence is a defining characteristic of hematopoietic stem cells, while their progeny have dramatic proliferative ability and inexorably move toward terminal differentiation. The quiescence of stem cells has been conjectured to be of critical biologic importance in protecting the stem cell compartment, which we directly assessed using mice engineered to be deficient in the G_1 checkpoint regulator, cyclin-dependent kinase inhibitor, $p21^{cip1/waf1}$ (p21). In the absence of p21, hematopoietic stem cell proliferation and absolute number were increased under normal homeostatic conditions. Exposing the animals to cell cycle–specific myelotoxic injury resulted in premature death due to hematopoietic cell depletion. Further, self-renewal of primitive cells was impaired in serially transplanted bone marrow from $p21^{-/-}$ mice, leading to hematopoietic failure. Therefore, p21 is the molecular switch governing the entry of stem cells into the cell cycle, and in its absence, increased cell cycling leads to stem cell exhaustion. Under conditions of stress, restricted cell cycling is crucial to prevent premature stem cell depletion and hematopoietic death.

High levels of production of mature blood cells are needed to replace their rapid turnover, yet it has been hypothesized that the proliferative activity of hematopoietic stem cells (HSCs) is highly restricted in order to prevent susceptibility to myelotoxic insult or consumption of the regenerative cell pool (*1–3*). Once cells embark on a path of high proliferation, they appear to have longevity limited to 1 to 3 months (*4*). It has therefore been hypothesized that hematopoietic tissue is organized so that stem cells are relatively quiescent, but their more differentiat-

ed offspring have extremely robust proliferative potential (*5*). The precise role of stem cell quiescence in the maintenance of the stem cell pool is unclear, and the molecular mechanisms governing it are not well defined.

Although it has been hypothesized that the quiescence of stem cells is protective, it poses practical problems for bone marrow transplantation (BMT) and stem cell gene therapy. Current methods for expanding the number of stem cells often involve the use of recombinant cytokines. However, these molecules have prodifferentiative as well as proliferative effects, and expansion often occurs at the expense of multipotentiality. Alternative strategies include the disruption of the dominant antiproliferative tone, which must be mediated proximately by molecular checkpoints in the cell cycle machinery. Cyclin-dependent kinase inhibitors (CKIs) participate in the sequential activation and inactivation of cyclin-dependent kinases, processes that are central to progression through the cell cycle (*6*, *7*). We and others have postulated that perturbation of these regulatory circuits may result in changes in stem cell proliferation, and indirect evidence has been generated through demonstration that antisense $p27^{Kip1}$ augments retroviral transduction of primitive hematopoietic cell populations (*8*). Targeted disruption of the gene encoding $p21^{cip1/waf1}$ (hereafter p21) in mice has resulted in cells that are impaired in their ability to achieve cell cycle arrest after irradiation (*9*, *10*), and antisense p21 has been shown to release human mesenchymal cells from G_0 (*11*). Therefore, p21 plays a role in at least some cell types in the transition out of the cell cycle and maintenance in G_0. However, in hematopoiesis, levels of p21 have not been shown to be increased in $CD34^+$ cells (*12*, *13*), and $p21^{-/-}$ mice have not been noted to have an altered hematologic profile (*9*, *10*). Further, bone marrow progenitor cells from $p21^{-/-}$ mice paradoxically have decreased proliferative ratios in response to cytokines (*14*, *15*). Yet we noted high levels of p21 mRNA when we assessed the quiescent stem cell–like fraction of bone marrow mononuclear cells. We therefore hypothesized that p21 plays distinct roles in subcompartments of the hematopoietic cascade, augmenting progenitor cell proliferation while inhibiting stem cell proliferation.

The direct impact of p21 on the stem cell compartment was assessed using mice engineered to be deficient in p21 (*16*). The cell cycling status of stem cells was determined using the RNA dye pyronin Y (PY) as a measure of quiescence among the lineage negative (lin^-) (*17*) and Hoechst 33342 (Ho) low-staining bone marrow cells (*18*). Cells from $p21^{-/-}$ animals consistently demonstrated a smaller fraction in the PY low portion of the continuum (Fig. 1) ($P = 0.005$, $n = 6$), which suggests that p21 does function to impede the entry of stem cells into the active cell cycle. Independently, rhodamine (Rho), a mitochondrial dye, and Ho were used to define the population of cells with low levels of metabolic activity and exclusion of Ho, corresponding to a quiescent stem cell pool (*19*). The Rho^{low}/Ho^{low} population of lin^- $Sca\text{-}1^+$ cells was also smaller in the $p21^{-/-}$ animals ($P = 0.07$, $n = 3$), confirming this observation.

To further define this issue, we injected −/− or +/+ mice with 200 mg of the antimetabolite 5-fluorouracil (5-FU) per kilogram of body weight (200 mg/kg) to selectively kill cycling cells (*20*, *21*). Marrow was harvested 1 day after 5-FU injection, and long-term culture or cobblestone area–forming cell (CAFC) assays were performed. These assays linearly correlate with in vivo repopulating potential (*22*, *23*) and were used here as a stem cell assay instead of competitive repopulation assays, given the lack of a congenic mouse strain with a 129/SV background. A significant reduction in CAFCs was noted after a pulse of 5-FU in the −/− group as compared with the +/+ group controls (60.5% versus 10.8%, $P = 0.0019$) (Fig. 2A).

When the animals were given 5-FU weekly as a challenge to assess the relative restriction on the cell cycle entry of primitive cells, the survival percentage in the −/− group was much lower than in littermate +/+ controls (10% versus 70% in 1 month, $P = 0.0054$) (Fig. 2B). To exclude the possible influence of toxicity to other tissues, we repopulated the hematopoietic system of lethally irradiated +/+ hosts with either +/+ or −/− bone marrow cells. One month after transplantation, we challenged the reconstituted animals with an identical protocol of sequential 5-FU treatment. A similar relative survival pattern was observed in mice carrying the −/− hematopoietic system, demonstrating markedly increased mortality as compared with those with a +/+ hematopoietic system ($P = 0.0089$). Therefore, death was due to hematopoietic and not other tissue sensitivity to the antimetabolite treatment. Thus, p21 restricts the entry of stem cells into the cell cycle and protects hematopoietic cells from destruction by cell cycle–dependent myelotoxic agents.

We next sought to determine whether the lack of p21 resulted in an increase in stem cell number in the basal state or in a decline due to more rapid depletion. The relative number of stem cells present in wild-type versus $p21^{-/-}$ mice was directly measured by limit-dilution CAFC assays. A significant increase in primitive cells in the $p21^{-/-}$ animals (Table 1, $P =$

[1]Experimental Hematology, AIDS Research Center, Massachusetts General Hospital Cancer Center, [2]Transplantation Biology Research Center, Massachusetts General Hospital, Harvard Medical School, Boston, MA, USA.

*To whom correspondence should be addressed at Massachusetts General Hospital, 149 13th Street, Room 5212, Boston, MA 02129, USA. E-mail: scadden.david@mgh.harvard.edu

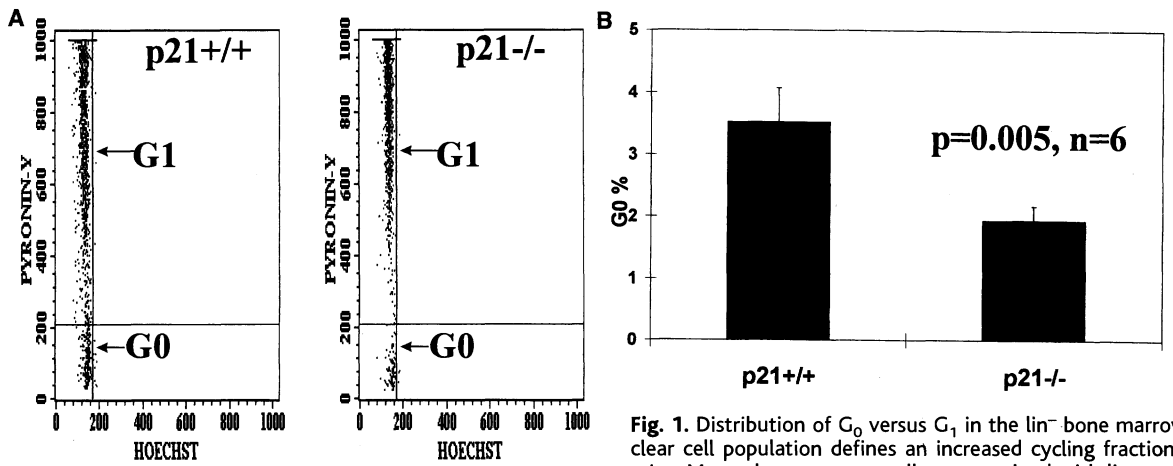

Fig. 1. Distribution of G_0 versus G_1 in the lin^- bone marrow mononuclear cell population defines an increased cycling fraction in $p21^{-/-}$ mice. Mouse bone marrow cells were stained with lineage antibodies, PY (RNA dye), and Ho (DNA dye). Lin^- cells were gated by means of a stringent parameter. Cells residing in G_0 appear at the bottom of the G_0/G_1 peak, and G_1 cells are the upper part as indicated (**A**). The average G_0% in lin^- Ho^{low} cells from six experiments is shown in the graph (**B**). Data represent the mean ± SE, $n = 6$, $P = 0.005$. One or two littermates of each genotype were analyzed in each experiment.

Table 1. Comparison of CAFCs scored at week 5 between $p21^{+/+}$ and $p21^{-/-}$ mice (per 10^5 bone marrow mononuclear cells) demonstrates increased numbers of stem cells. Each pair was pooled from two or three −/− or +/+ littermate mice in each experiment. Each data point was generated from three to five limiting dilutions, and data were analyzed with the paired *t* test.

Experiment number	$p21^{+/+}$	$p21^{-/-}$
1	2.88	4.98
2	2.41	5.29
3	0.83	1.06
4	0.58	0.92
5	0.18	0.49
6	0.87	1.33
7	0.32	1.25
Mean	1.15	2.19
P value, paired *t* test	0.0393	0.0393

Table 2. Comparison of CFCs between $p21^{+/+}$ and $p21^{-/-}$ mice (per 10^4 bone marrow mononuclear cells) indicates no difference in progenitors. Data represent colony-forming ability at day 10. Each pair was pooled from two or three −/− or +/+ littermate mice in each experiment. Each data point was generated from at least four replicates, and data were analyzed with the paired *t* test.

Experiment number	$p21^{+/+}$	$p21^{-/-}$
1	66.65	50.00
2	76.25	35.00
3	60.00	45.00
4	55.00	80.00
5	51.84	56.50
6	42.33	35.67
7	32.67	35.00
Mean	54.96	48.17
P value, paired *t* test	0.4189	0.4189

Table 3. Comparison of total mononuclear cell number per bone marrow harvest between $p21^{+/+}$ and $p21^{-/-}$ mice indicates no difference in cellularity. Each data point represents the mean from one to three –/– or +/+ littermate mice in each experiment. The total cell number ($\times 10^7$ per femur pair) was counted from each harvest, and data were analyzed using the paired *t* test.

Experiment number	$p21^{+/+}$	$p21^{-/-}$
1	1.4	1.3
2	1.58	1.76
3	2.5	2.08
4	1.5	1.5
5	1.53	1.27
6	1.29	2.14
Mean	1.63	1.68
P value, paired *t* test	0.8284	0.8284

0.0393, $n = 7$) was noted. Thus, p21 provides a dominant negative effect, which is sufficient to inhibit stem cell cycling. In the absence of p21, the inhibition is alleviated, leading to an expansion of the primitive cell pool under resting conditions. In contrast, no significant differences in colony-forming cells (CFCs), bone marrow cellularity, or white blood cells were noted (Tables 2 through 4), implying that p21 has a differentiation stage–specific function in HSCs. The paradoxic pro-proliferative effect of p21 in more mature progenitors observed by others may balance the inhibitory influence of p21 on stem cells (*14*, *15*). This apparent dichotomy may reflect the complex biochemical role p21 has been noted to play as either a requisite participant in the formation of the cyclin–cyclin-dependent kinase complex that is necessary for the movement of the cell through late G_1 into S, or as a CKI, inhibiting entry into S phase (*24*). We speculate that p21 plays a central role in determining the known differences in sensitivity to proliferative stimuli between stem cells and progenitor cells and that the opposing effects of p21 are selectively manifest based on the differentiation status of the hematopoietic cell.

The expansion of stem cells under normal homeostatic conditions may or may not reflect a capacity to self-renew under conditions of stress. The cytokine milieu dramatically changes during stress, including the elaboration of cytokines such as granulocyte-macrophage colony-stimulating factor (GM-CSF), granulocyte-CSF (G-CSF), and interleukin-3 (IL-3) with strong pro-differentiative properties. We hypothesized that the outcome of enhanced proliferation of the stem cell compartment under such conditions will markedly differ from normal homeostasis, and we directly assessed stem cell self-renewal capability using a serial transplantation approach (*25*–*28*). Bone marrow from 10 male animals of each genotype was individually transplanted into lethally irradiated female mice. Two to 4 months after engraftment, 1×10^6 to 2×10^6 bone marrow mononuclear cells from the transplanted recipients were used as donor cells for a lethally irradiated host, and the same procedure was repeated sequentially. Recipient animals began to die after the third serial transplant, and marked differential survival in the group was noted (Fig. 3A). No −/− transplanted animals survived after the fifth transplant, whereas the +/+ transplanted animals had a 50% survival 1 month after that transplant. To confirm the paucity of stem cells in −/− transplanted mice, we used two different doses of cells from the fourth transplant to rescue lethally irradiated hosts. The two irradiation protection experiments at different doses confirmed the significantly poorer ability of cells from the −/− group to rescue irradiated mice (Fig. 3B). We observed an approximately 100% contribution from the original donor $p21^{-/-}$ or $p21^{+/+}$ cells in hosts examined after each transplant by means of semiquantitative Y chromosome–specific (Sry) polymerase chain reaction (PCR) and p21 genotyping PCR (Fig. 3C).

To evaluate whether the transplantation data could be affected by altered homing of stem cells in the absence of p21, we directly measured the localization of ex vivo fluorescently labeled $p21^{-/-}$ and $p21^{+/+}$ bone marrow cells with carboxy fluorescein diacetate succinimidyl

Table 4. Comparison of blood cell counts between $p21^{+/+}$ and $p21^{-/-}$ mice ($n = 10$, mean ± SD) indicates no significant difference in mature cell populations. Blood was collected by tail bleeding. All the blood counts were performed and analyzed using the *t* test for two samples with the same variance. WBCs, white blood cells; RBCs, red blood cells; PLTs, platelets.

	WBCs ($\times 10^3/\mu l$)	RBCs ($\times 10^6/\mu l$)	PLTs ($\times 10^3/\mu l$)
$p21^{+/+}$	5.38 ± 2.95	9.08 ± 0.86	444.60 ± 55.99
$p21^{-/-}$	7.48 ± 1.83	9.38 ± 0.96	510.10 ± 141.65
P value	0.0670	0.2290	0.0950

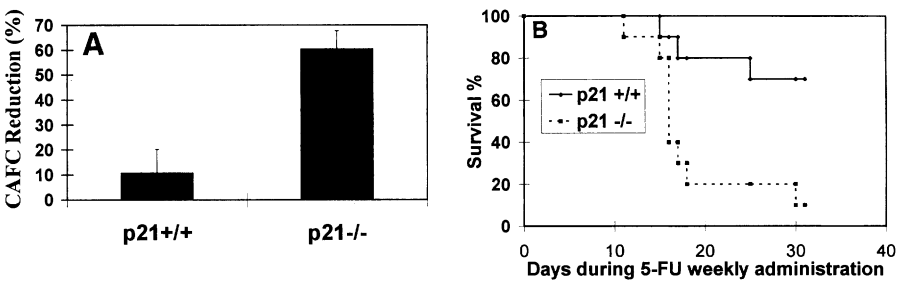

Fig. 2. Response of $p21^{-/-}$ mice to 5-FU treatment in vivo demonstrates a higher cycling status and increased sensitivity to toxic injury. (**A**) CAFC reduction after a 5-FU pulse. A single i.v. injection of 5-FU at the dose of 200 mg/kg was performed, and cells for LTC with limiting dilution were obtained 1 day after the injection. CAFCs were counted at week 5. The *y* axis values = [(CAFCs from untreated mice – CAFCs from 5-FU–treated mice)/(CAFCs from untreated mice)] × 100%. Data represent the mean from three independent experiments. Three littermates from each genotype were used in each experiment, and three to five limiting dilutions were applied for each sample. Student's *t* test was used to analyze the data ($n = 3$, $P = 0.0019$). (**B**) Survival outcome after sequential 5-FU treatment. 5-FU was administered i.p. weekly at a dose of 150 mg/kg, and the survival rates of the groups were defined. Results were analyzed with a log-rank nonparametric test and expressed as Kaplan-Meier Survival curves ($n = 10$, $P = 0.0054$).

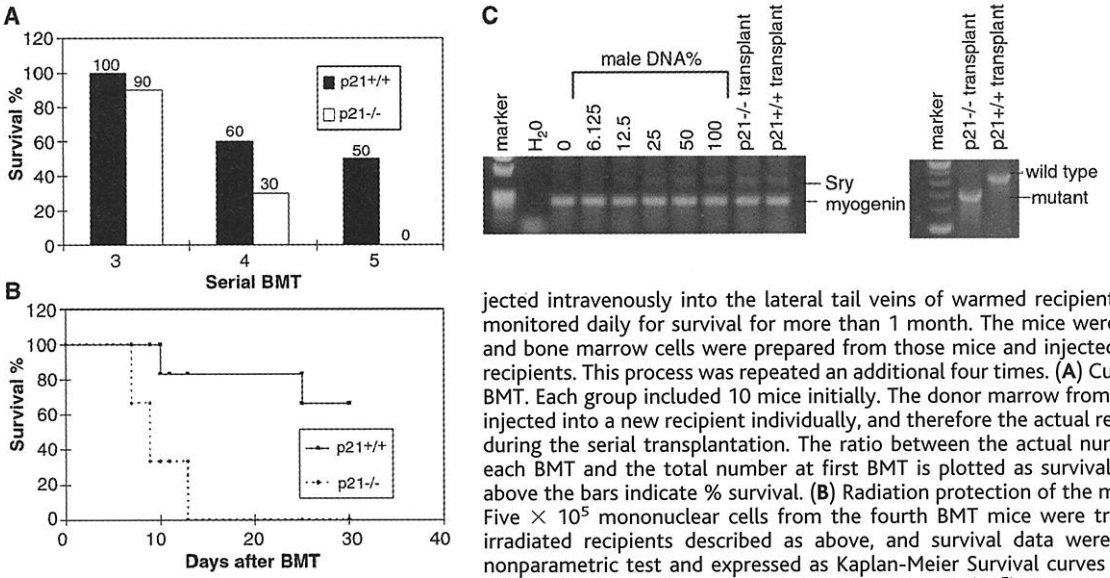

Fig. 3. Animal survival after serial BMT demonstrates reduced self-renewal of hematopoietic potential. Male mice were used as marrow donors. Female recipient mice were lethally irradiated with 10 Gy of whole-body irradiation at 5.96 Gy/min. Two million nucleated cells were injected intravenously into the lateral tail veins of warmed recipient mice. Recipient mice were monitored daily for survival for more than 1 month. The mice were killed after 2 to 4 months, and bone marrow cells were prepared from those mice and injected into new female irradiated recipients. This process was repeated an additional four times. (**A**) Cumulative survival after serial BMT. Each group included 10 mice initially. The donor marrow from the previous transplant was injected into a new recipient individually, and therefore the actual recipient number was reduced during the serial transplantation. The ratio between the actual number of surviving animals at each BMT and the total number at first BMT is plotted as survival % (*y* axis value). Numbers above the bars indicate % survival. (**B**) Radiation protection of the marrow from the fourth BMT. Five × 10^5 mononuclear cells from the fourth BMT mice were transplanted into the lethally irradiated recipients described as above, and survival data were analyzed using a log-rank nonparametric test and expressed as Kaplan-Meier Survival curves (n = 6 for each group, P = 0.002). Similar results were obtained at lower doses (10^5) of donor cells (n = 10 for each group, P = 0.008, curve not shown). (**C**) Donor contribution monitored by PCR. The contribution of the original donor cells was monitored by a PCR-based semiquantitative analysis for a Y chromosome–specific sequence (Sry), using an aliquot of marrow sample from each transplant. DNA was prepared from donor cells collected at the fourth transplant, and 200 ng was used for the PCR analysis. Two percent agrose gel was used to display the PCR products. The left gel shows the positive controls, which were mixed with male and female DNA at the ratios indicated. The complete contribution from donor cells was further confirmed by p21 genotyping PCR, shown in the right gel. Similar results were obtained from the first, second, and third transplants (data not shown in figure).

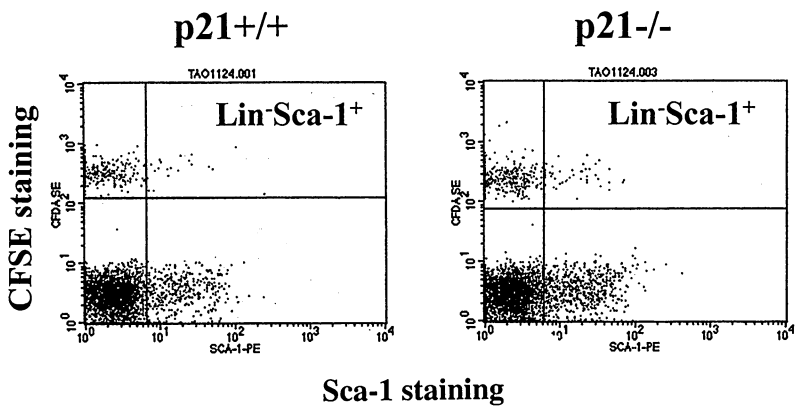

Fig. 4. p21$^{-/-}$ stem cell depletion is not due to altered bone marrow homing. Donor bone marrow cells were stained with the cytoplasmic dye CFSE and intravenously injected into lethally irradiated mice. Bone marrow and the spleen were harvested 9 hours after injection, and nucleated cells were stained with Sca-1 and lin antibodies and analyzed by flow cytometry. Two or three littermates of each genotype were analyzed in each experiment. Data shown are for bone marrow cells from one of two experiments with similar results.

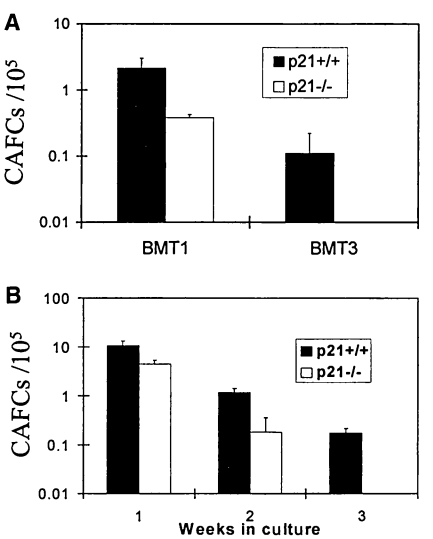

Fig. 5. CAFCs over the course of serial BMT confirm stem cell exhaustion. LTC with limiting dilution was performed on the donor cells of each transplant to quantify the frequencies of hematopoietic progenitors and stem cells. Normal untransplanted marrow was used as a control to ensure the quality of the stroma and the comparability of the experiments at different times. Data are represented as the mean ± SD and graphed as log scales on the *y* axis. All *P* values are less than 0.05 (−/− versus +/+). (**A**) CAFCs at week 5 from the first and third transplants. (**B**) CAFCs at the indicated weeks from the fourth transplant.

diester (CFSE) (*29*) after transplantation. The fraction of mononuclear cells or of lin$^-$, Sca-1$^+$ cells homing to either bone marrow or the spleen was the same for the −/− and +/+ mice (Fig. 4).

These functional in vivo parameters of stem cell function were corroborated with quantitative in vitro measures of function of the primitive cell compartment. CAFCs scored at week 5 from −/− mice were completely exhausted after the third transplant, whereas detectable CAFCs were still noted in the +/+ group (Fig. 5A). Although an absence of CAFCs after 4 weeks was observed in both the +/+ and −/− groups from the fourth transplant, early CAFCs (scored at week 2 and 3) reflecting short-term repopulating cells (*22*, *23*), demonstrated a significant difference (Fig. 5B). The CAFCs in −/− transplant recipients dampened to zero after 2 weeks, whereas the CAFCs in +/+ transplant recipients remained detectable at 3 weeks. The levels of CAFCs in −/− mice were also significantly lower than in the +/+ group [all P values <0.05 (Fig. 5B)].

Stem cell quiescence is therefore critical for both protection from myelotoxic injury and preservation of the stem cell pool under conditions of stress. p21$^{-/-}$ animals exhibit increased stem cell numbers under homeostatic conditions, without the ability to appropriately self-renew when transplanted. The distinction in stem cell generation between these different conditions may have several potential explanations. Telomere shortening with the demands of transplantation leading to cell death is possible (*30*) as is enhanced apoptosis in the −/− state

(*31*), although the latter would be expected to effect basal as well as posttransplant cells. Differentiation of HSCs may be directly inhibited by p21, thereby enhancing differentiation in the −/− animals, but a pro-differentiative role for p21 has been described in all but terminally differentiated cells (*13*, *32*). Rather, we propose a model in which the dominant inhibitory tone of p21 on cell cycle entry blunts the response to inflammatory cytokines, maintaining cells in G_0 thereby precluding accomplishment of the differentiation program. Simply conceived, without the entry into the cell cycle, the differentiative effects of cytokines cannot proceed. This effect on the cell cycle, evident in regulating the size of the stem cell pool under normal homeostasis, is crucial in protecting stem cells from being consumed under conditions of stress. Therefore, cell cycle control is itself a critical determinant of stem cell pool persistence in vivo.

The ability of a single molecule, p21, to dictate stem cell pool kinetics in vivo suggests that p21 may be an important target molecule in efforts to manipulate stem cell proliferation ex vivo. Relieving p21-enforced inhibition of the cell cycle in the absence of pro-differentiative cytokines ex vivo may permit direct analysis of whether stem cell proliferation is necessarily linked to differentiation and will assess the validity of the concept of stem cell expansion.

References and Notes

1. P. Mauch, J. Ferrara, S. Hellman, *Bone Marrow Transplant.* **4**, 601 (1989).
2. P. Mauch *et al.*, *Int. J. Radiat. Oncol. Biol. Phys.* **31**, 1319 (1995).
3. R. V. Gardner, C. M. Astle, D. E. Harrison, *Exp. Hematol.* **25**, 495 (1997).
4. N. J. Drize, J. R. Keller, J. L. Chertkov, *Blood* **88**, 2927 (1996).
5. M. Ogawa, *Blood* **81**, 2844 (1993).
6. C. J. Sherr, *Cell* **79**, 551 (1994).
7. _____ and J. M. Roberts, *Genes Dev.* **9**, 1149 (1995).
8. M. A. Dao and J. A. Nolta, *Exp. Hematol.* **26**, 686 (1998).
9. J. Brugarolas *et al.*, *Nature* **377**, 552 (1995).
10. C. Deng, P. Zhang, J. W. Harper, S. J. Elledge, P. Leder, *Cell* **82**, 675 (1995).
11. M. Nakanishi *et al.*, *Proc. Natl. Acad. Sci. U.S.A.* **92**, 4352 (1995).
12. T. Taniguchi *et al.*, *Blood* **93**, 4167 (1999).
13. B. Yaroslavskiy, S. Watkins, A. D. Donnenberg, T. J. Patton, R. A. Steinman, *Blood* **93**, 2907 (1999).
14. C. Mantel *et al.*, *Blood* **88**, 3710 (1996).
15. S. E. Braun *et al.*, *Blood Cells Mol. Dis.* **24**, 138 (1998).
16. Experimental methods were as follows. **Generation of homozygous mice:** We obtained heterozygote 129/SV $p21^{+/-}$ mice (9) from the laboratory of Tyler Jacks (MIT, Boston) under the permission of the Subcommittee on Research Animal Care of the Massachusetts General Hospital (MGH). Mice were housed in sterilized microisolator cages and received autoclaved food and drinking water at the MGH animal core facility. The inbred 129/SV heterozygotes (+/–) were bred to yield homozygous and wild-type offspring. The littermates from the same +/– parents were used in each experiment. **Mouse genotyping**: Genotyping was done by DNA PCR. Briefly, genomic DNA was isolated from tail biopsy and analyzed by amplification using three primers: p21 +116F (AAG CCT TGA TTC TGA TGT GGG C), p21 –135 (TGA CGA AGT CAA AGT TCC ACC G), and Neo19+ (GCT ATC AGG ACA TAG CGT TGG C). p21 +116F was involved in the amplification of both mutant and wild-type alleles. The conditions for thermocycling were as follows: Step 1, 94°C for 4 min; step 2, 94°C for 1 min, 64°C for 1 min, and 72°C for 2 min, for 40 cycles; step 3, 72°C for 2 min. Diagnostic mutant and wild-type bands were 750 base pairs (bp) and 900 bp, respectively, on 2.0% agarose gel electrophoresis. **Bone marrow sampling:** Mouse bone marrow was obtained from 8- to 12-week-old animals from each group (−/− and +/+) that had been killed with CO_2. The marrow cell suspensions were flushed from femurs and tibias, filtered with 100-mesh nylon cloth (Sefar America, Kansas City, MO), and stored on ice until use. **Flow cytometric analysis:** Flow cytometry was used to quantify the cell cycle status in the stem cell compartment. Bone marrow nucleated cells were incubated with DNA dye Ho (1.67 μmol/liter) and RNA dye PY (1 μg/ml) at 37°C for 45 min, respectively (*17*) then labeled with biotinylated antilineage antibodies [CD3, CD4, CD8, B220, Gr-1, Mac-1 (Caltag, Burlingame, CA), and TER-119 (Pharmigen)] and strepavidin–fluorescein isothiocyanate. Flow cytometry was performed on FACSVantage Instruments (Becton Dickinson). **Colony forming assay:** Bone marrow nuclear cells were cultured in 0.8% methylcellulose; 30% fetal bovine serum; 1% bovine serum albumin; 0.1 mM 2-mercaptoethanol; and 2.0 mM L-glutamine of α–minimum essential medium (α-MEM) semisolid matrix culture medium (StemCell Technologies, Vancouver, BC), with cytokine combinations of human SCF (hu-SCF) (50 ng/ml) (R & D System, Minneapolis, MN), murine IL-3 (mu-IL-3) (20 ng/ml) (Genzyme), hu-IL-6 (20 ng/ml) (Genzyme), hu-G-CSF (50 ng/ml) (R & D System), hu-GM-CSF (20 ng/ml) (R & D System) and hu-Epo (2 U/ml) (Amgen). Cells were plated at 20,000 cells per 200 μl per well into 48-well plates and placed at 37°C in 5% CO_2. At day 10, myeloid and erythroid colonies were scored, totaled, and reported as CFCs. **Long-term culture with limiting dilution:** To quantify the stem cells, we adapted the CAFC assay (*23*) with minor modifications as follows. To prepare stromal layers, murine bone marrow nucleated cells were cultured at 33°C in long-term culture (LTC) medium [α-MEM with 12.5% house serum, 12.5% fetal bovine serum, 0.2 mM I-inositol, 20 mM folic acid, 10^{-4} M 2-mercaptoethanol, 2 mM L-glutamine, and 10^{-6} M hydrocortisone]. After 2 weeks, confluent stromal layers were trypsinized, irradiated [15 gray (Gy)], and subcultured in 96-well flat-bottomed plates at a density of 2.5×10^4 per well. Cultures were then seeded with serially diluted single-cell suspensions of femoral marrow in the same medium. Marrow pooled from 2 to 10 animals of each type was seeded at twofold dilutions (10^5 - 1562 cells per well) for nucleated bone marrow cells. Cultures were very gently refed with 50 ml of medium after semidepletion weekly, and the CAFCs and/or blast colonies (*23*, *33*) were scored until the sixth week. **5-FU exposure in vivo:** The antimetabolite 5-FU was used to selectively deplete cycling cells in vivo. 5-FU was administered intraperitoneally (i.p.) weekly at a dose of 150 mg/kg, and the survival rates of the groups were defined. To more specifically test the effect of p21 on hematopoietic cells, we transplanted bone marrow cells from $p21^{-/-}$ or $p21^{+/+}$ animals into lethally irradiated mice of the same genetic background ($p21^{+/+}$, 129/SV, 8 weeks old, Jackson Laboratory), allowing the hematopoietic and immune system to repopulate for 1 month, and then observed the effects of 5-FU on those animals. To test the sensitivities of primitive hematopoietic cells, a single intravenous (i.v.) injection of 5-FU at a dose of 200 mg/kg was administered, and cells for LTC with limiting dilution were obtained 1 day after the injection. **Serial BMT:** Serial BMT (*25–28*) was used to evaluate the ability of stem cells to self-renew. Male mice (8 to 12 weeks old) were used as marrow donors, and the marrow cells were prepared as above. Female recipient mice (8 to 10 weeks old, 129/SV, Jackson Laboratory) were lethally irradiated with a Mark 1-Model 25 ^{137}Cesium Irradiator (JL Shepherd and Associates, San Fernando, CA) with 10 Gy of whole-body irradiation at 5.96 Gy/min. One to two million nucleated cells in 1 ml of 199 Medium were injected intravenously through 27-gauge needles into the lateral tail veins of warmed recipient mice. Recipient mice were monitored daily for survival for more than 30 days, which is the period of time in which stem cells have been noted by others to account for hematopoietic recovery after lethal irradiation (*34*). The mice were killed at 2 to 4 months, and bone marrow cells were prepared from those mice and injected into new female recipients. This process was repeated for four sequential transplants, with survival frequency plotted for each group. LTC with limiting dilution described above was performed on the donor cells of each transplant to quantify the frequencies of hematopoietic progenitors and stem cells. **Semiquantitative DNA PCR for the Y chromosome:** The contribution of the original donor cells was monitored by a PCR-based semiquantitative analysis for a Y chromosome specific sequence (Sry) (*35*), using an aliquot of each marrow sample described below. Briefly, DNA from bone marrow cells was isolated with a Puregene kit (Gentra System, Research Triangle Park, NC) according to the manufacturer's instructions. Two hundred nanograms of DNA was applied to the PCR reaction. The sequences for the PCR primers were as follows (5′-3′). Sry primers: TCA TGA GAC TGC CAA CCA CAG and CAT GAC CAC CAC CAC CAC CAA; myogenin primers: TTA CGT CCA TCG TGG ACA GC and TGG GCT GGG TGT TAG TCT TA. The PCR cycles were for 5 min at 94°C and for 35 cycles at 94°C for 10 s, then at 65°C for 30 s, followed by 5 min at 72°C. A linear relation between the ratios of male genomic DNA to the total amount of DNA and the signal intensities of the PCR product was plotted simultaneously in order to quantify the contribution of donor cells. **Homing assay**: Donor marrow nucleated cells were stained with the cytoplasmic dye CFDA SE (CFSE) according to the manufacturer's instructions (Molecular Probes, Eugene, OR), and 2×10^7 CFSE-stained cells was injected into lethally irradiated recipient mice. The spleen and bone marrow were harvested 9 hours after injection, and cells were stained with lineage markers and antibody to Sca-1 before flow cytometric analysis. **Statistical analysis:** Results from survival experiments were analyzed with a log-rank nonparametric test and expressed as Kaplan-Meier Survival curves (*36*). The significance of the difference between groups in the in vitro culture was evaluated by analysis of variance, followed by a two-tailed Student's *t* test.
17. A. Gothot *et al.*, *Blood* **90**, 4384 (1997).
18. A. Gothot *et al.*, *Exp. Hematol.* **26**, 562 (1998).
19. N. S. Wolf, A. Kone, G. V. Priestley, S. H. Bartelmez, *Exp. Hematol.* **21**, 614 (1993).
20. A. C. Berardi, A. Wang, J. D. Levine, P. Lopez, D. T. Scadden, *Science* **267**, 104 (1995).
21. C. Lerner and D. E. Harrison, *Exp. Hematol.* **18**, 114 (1990).
22. R. E. Ploemacher, J. P. van der Sluijs, C. A. van Beurden, M. R. Baert, P. L. Chan, *Blood* **78**, 2527 (1991).
23. R. E. Ploemacher, J. P. van der Sluijs, J. S. Voerman, N. H. Brons, *Blood* **74**, 2755 (1989).
24. J. LaBaer *et al.*, *Genes Dev.* **11**, 847 (1997).
25. D. E. Harrison, C. M. Astle, J. A. Delaittre, *J. Exp. Med.* **147**, 1526 (1978).
26. D. E. Harrison, *Blood* **55**, 77 (1980).
27. _____ and C. M. Astle, *J. Exp. Med.* **156**, 1767 (1982).
28. D. E. Harrison, M. Stone, C. M. Astle, *J. Exp. Med.* **172**, 431 (1990).
29. T. Holyoake, X. Jiang, C. Eaves, A. Eaves, *Blood* **94**, 2056 (1999).
30. J. M. Zijlmans *et al.*, *Proc. Natl. Acad. Sci. U.S.A.* **94**, 7423 (1997).
31. J. Wang and K. Walsh, *Science* **273**, 359 (1996).
32. F. Di Cunto *et al.*, *Science* **280**, 1069 (1998).
33. C. E. Muller-Sieburg and R. Riblet, *J. Exp. Med.* **183**, 1141 (1996).
34. N. Uchida, H. L. Aguila, W. H. Fleming, L. Jerabek, I. L. Weissman, *Blood* **83**, 3758 (1994).
35. A. M. Muller and E. A. Dzierzak, *Development* **118**, 1343 (1993).
36. K. Grzegorzewski *et al.*, *J. Exp. Med.* **180**, 1047 (1994).

37. The authors thank T. Jacks and J. Brugarolas for $p21^{+/-}$ mice and D. Haber and F. Preffer for helpful discussions. Supported by DARPA grants HL44851 and DK50234 and by the Richard Saltonstall Charitable Foundation (D.T.S.), grants AI07387 and DK02761 (T.C.) and HL49915 (M.S.).

8 December 1999; accepted 27 January 2000